OBSERVATIONAL STUDIES OF MOUNTAIN GENERATED MOMENTUM FLUXES

Klaus P. Hoinka
Institute of Atmospheric Physics, DFVLR
D-8031 Oberpfaffenhofen
Federal Republic of Germany

Summary: The present paper summarises efforts to determine momentum flux values derived from observational data taken by aircraft over the last two decades. It provides a short derivation of the equation which is commonly used to calculate the momentum flux from observed data. Subsequently the methods of measuring and of treating the measured data are described briefly. Finally it discusses the problems of determining momentum fluxes based on observed data.

1. INTRODUCTION

The exchange of momentum between the atmosphere and the earth is one of the central concerns of meteorology. Mountains play an important role in affecting the atmospheric momentum budget in several ways: there is a drag due to purely frictional effects because the mountains are rough; secondly the mountains cause the flow to decelerate because they stand as barriers in the flow; thirdly they generate waves above and on the lee side which are sometimes associated with turbulence; and finally they induce and intensify diabatic processes which may in turn influence the momentum budget. All these processes cause momentum transfer between the atmosphere and its wavy lower surface by extracting a significant amount of momentum from the mean flow.

In 1972 Lilly pointed out that '...the magnitude and distribution of mountain-induced drag on the atmosphere is unknown...'. How far is Lilly's statement correct today, after much theoretical and observational work has been done trying to fill this gap? The purpose of this paper is to summarise the results on mountain generated momentum fluxes obtained from observations taken during the last 20 years.

Until the end of the 1960's observational data gathered by aircraft were used to determine the flow fields and structures of airflow over and around mountains. Of particular interest were the determination of the

wavelength and wave amplitude of lee waves and the comparison of the observational results with theoretical approaches. Several flight programmes and single measurements were performed to gather relevant data. However, with the available technology it was only possible to measure the thermal structure of the troposphere from which to derive the flow behaviour.

According to the theory, the mountain drag force is transmitted upwards from each atmospheric layer in turn by wave-induced momentum fluxes. This vertical momentum flux can be estimated from measurements of instrumented aircraft flying above the mountain. About 20 years ago it was possible to make these kind of in-situ measurements of the wind vector down to turbulence scales using airborne systems. In the following years probably the most fruitful observations have been carried out from these instrumented aircraft, especially those equipped with high grade motion sensing systems. Several field experiments document this progress. They comprised single and co-ordinated series of measurements.

In the subsequent sections we present: first, a brief derivation of the momentum flux terms which must be calculated using observational data; next we describe briefly the instruments and methods to measure the velocities; then we describe the methods of treating the data and subsequently we present a summary of efforts to determine momentum fluxes calculated from aircraft data; then we discuss turbulence data taken above mountainous terrain; and finally we outline general problems in calculating mountain generated momentum fluxes.

2. THE MOMENTUM FLUX

This section gives a brief derivation of the momentum flux term. It describes momentum losses due to gravity waves generated by mountains and due to turbulence. This term can then be used to calculate the momemtum flux from observational data. To illustrate the difference between momentum losses due to turbulence and those due to waves we start with the equation of momentum for two-dimensional flow:

$$\frac{\partial}{\partial t}(\rho u) = -\frac{\partial}{\partial x}(\rho uu) - \frac{\partial}{\partial z}(\rho uw) - \frac{\partial p}{\partial x} + f\, v\, \rho. \qquad (1)$$

It is convenient to perform the decomposition $\phi = \overline{\phi} + \phi^{*}$ where ϕ represents any one of the dependent variables and

$$\bar{\phi} = \frac{1}{\Delta t\ \Delta x\ \Delta z} \int_{t}^{t+\Delta t} \int_{x}^{x+\Delta x} \int_{z}^{z+\Delta z} \phi \, dt \, dx \, dz. \qquad (2)$$

Thus $\bar{\phi}$ represents the average of ϕ over a finite time increment Δt and space interval Δx, Δz. In a numerical model Δx and Δz represent the model grid intervals and Δt the timestep. Therefore $\bar{\phi}$ is called a 'grid-volume average'. For observations and measurements the Δt might be the sampling time of data and the Δx and Δz the corresponding length scale.

The next step is to perform an integration of (1) over Δx, Δz and Δt and assuming that $|\rho^*|/(\bar{\rho}) \approx |\rho^*|/(\rho_o) \ll 1$, where $\rho_o(z)$ is defined as a synoptic scale density. The grid-volume averaged $\bar{\phi}$ can now further be decomposed by $\bar{\phi} = \phi_o + \phi'$ into a 'layer-domain-averaged' variable $\phi_o(z)$ and its deviation ϕ'

$$\phi_o = \frac{1}{L} \int_L \bar{\phi} \, dx. \qquad (3)$$

After another integration, but now over the domain L, yields

$$\frac{\partial}{\partial t}(\rho_o u_o) = -\int_L \frac{\partial}{\partial x}(\rho_o \bar{u}\,\bar{u})\,dx - \int_L \frac{\partial}{\partial x}(\rho_o \overline{u^* u^*})\,dx - \int_L \frac{\partial p'}{\partial x}\,dx \qquad (4)$$
$$- \frac{\partial}{\partial z}\int_L (\rho_o \bar{u}\,\bar{w} + \rho_o \overline{u^* w^*})\,dx + \int_L f\, v'\, \rho_o\, dx$$

which is the budget equation for the domain-averaged horizontal momentum. The terms on the right hand side represent, from left to right, the horizontal flux of horizontal momentum, the subgrid-scale horizontal eddy flux, the flux due to pressure gradient forces, the sum of the vertical flux of horizontal momentum and the subgrid-scale vertical eddy flux, and the flux due to Coriolis force. When the vertical eddy stress convergence (integral part of the fourth term) is substantial and positive, as is believed to be common in gravity waves in middle latitudes, it represents a force acting against the air flow, and therefore acts as a sink of atmospheric kinetic energy. In a stably stratified atmosphere however, gravity waves are capable of transporting momentum substantial distances between its sources and sinks, without necessarily affecting the intervening layers, i.e. this term may be substantial, but its height derivative may vanish.

Assuming a steady state and applying the lower boundary condition $w'(x,h) = u'(x,h)dh/dx$, (4) is integrated vertically from the orography $z = h(x)$ to an arbitrary height $z = H$

$$- \int_L p'(x,h) \frac{dh}{dx} dx = + \int_L (\rho_o \bar{u}\,\bar{w}) dx + \int_L (\rho_o \overline{u^* w^*}) dx \qquad (5)$$

$$- \int_L \int_{h(x)}^{H} (f\, v' \rho_o) dz\, dx + \Big[\int_{h(x)}^{H} (\rho_o \bar{u}\,\bar{u} + \rho_o \overline{u^* u^*} + p') dz \Big]_{x=-L/2}^{x=+L/2}.$$

Far enough up and downstream of a two-dimensional barrier ($L/2 \to \pm \infty$) the last term on the right hand side vanishes. Assuming that w_o vanishes, the first term on the right hand side can be rewritten as

$$\int_L \rho_o (\bar{u}\,\bar{w}) dx = \int_L \rho_o (u'w') dx. \qquad (6)$$

Finally, (5) yields

$$- \int_{-\infty}^{+\infty} p'(x,h) \frac{dh}{dx} dx = + \int_{-\infty}^{+\infty} (\rho_o u'w') dx + \int_{-\infty}^{+\infty} (\rho_o \overline{u^* w^*}) dx + \int_{-\infty}^{+\infty} (f\, v' \rho_o \eta) dx \qquad (7)$$

with η the vertical displacement of a fluid particle from its undisturbed level. The left side of (7) represents the net drag on the mountain resulting from the horizontal surface pressure difference

$$D = - \int_{-\infty}^{+\infty} p'(x,h) \frac{dh}{dx} dx = \int_{-\infty}^{+\infty} h(x) \frac{\partial p'}{\partial x} dx. \qquad (8)$$

This drag is called the 'mountain drag', 'surface pressure drag' or 'form drag'. The right-hand side of Eq.(7) describes the vertical flux of horizontal momentum through a horizontal plane at an arbitrary height. The terms represent, from left to right, the momentum flux due to gravity waves, the momentum flux due to turbulence generated by subgrid-scale motion and the excess Coriolis force acting between the undisturbed and the lifted stream surface. The first term on the right hand side shows the so-called 'wave drag' M purely due to gravity waves. The second term might be called the 'turbulent drag' T

$$T = \int_{-\infty}^{+\infty} (\rho_o \overline{u^* w^*}) \, dx. \qquad (9)$$

At this point it becomes obvious that the subdivision into turbulence and wave generated momentum flux depends strongly on the definition of 'Δx', 'Δz' and 'Δt'. All motion with characteristic scale smaller than Δx is defined as turbulent motion and all that beyond this limit is considered to be wave motion.

In a rotating system the last term on the right hand side of (7) does not vanish, it represents the net Coriolis force excerted on a fluid particle. The sum of the first and third term represents the wave drag due to gravity-inertia waves. Bretherton (1969) pointed out that in plane gravity-inertial waves a vertical displacement η is correlated with a displacement in the x-direction and hence with a velocity v in the y-direction. For reasonable wind speeds, Smith (1979) has shown that for mountain ranges such as the Alps the earth's rotation is important but not dominant. Smith showed that the drag of a mountain with a half-width of 50 km in a flow of 10 m s^{-1}, including Coriolis effects, is about 20% larger in magnitude than its value in the non-rotating case.

The vertical flux of horizontal momentum in non-turbulent non-rotating wave motion is given by

$$M = \int_{-\infty}^{+\infty} (\rho_o u'w') \, dx. \qquad (10)$$

The dimensions are kg s^{-2} or N m^{-1}. It is clear that the influence of the mountain vanishes far upstream as well as downstream. Data can only by observed over a limited area, e.g. a distance A, hoping that over this distance the influence of the barrier vanishes upstream as well as downstream. The approximate width of a mountain range, such as the Alps or the Rocky Mountains, is about 100 km. For these mountains A might be between 200 and 300 km. For comparisons it is convenient to consider the flux values over a standard length, e.g. one meter. The momentum flux is then approximated by

$$M = \frac{1}{A} \int_A (\rho_o u'w') \, dx \qquad (11)$$

with dimensions of N m^{-2} which is equal to one Pa or 10 dynes cm^{-2}.

To illustrate the relation between the wave pattern and its associated momentum flux we consider the horizontal momentum ρu being transported by the vertical velocity w. For simplicity the momentum per unit mass is considered which is represented by the horizontal wind component u. In Fig.1 (a) the same amount of momentum is transported upward at the rear of the ridge line as is transported downward in front of the ridge line. Because the phaselines have no vertical tilt no momentum is transported vertically. Frequently the wave front tilts upwind (b) as is common where there are gravity waves. Then, the upward transfer of horizontal momentum in the upwind part of the wave is generally less than the downward transfer in the downwind part of the wave. Consequently the net effect of this wave type is to achieve a downward flux of momentum. It is clear that as soon as the wave front is tilted vertically downstream the momentum flux is greater than zero which means that the flux is directed upwards (c).

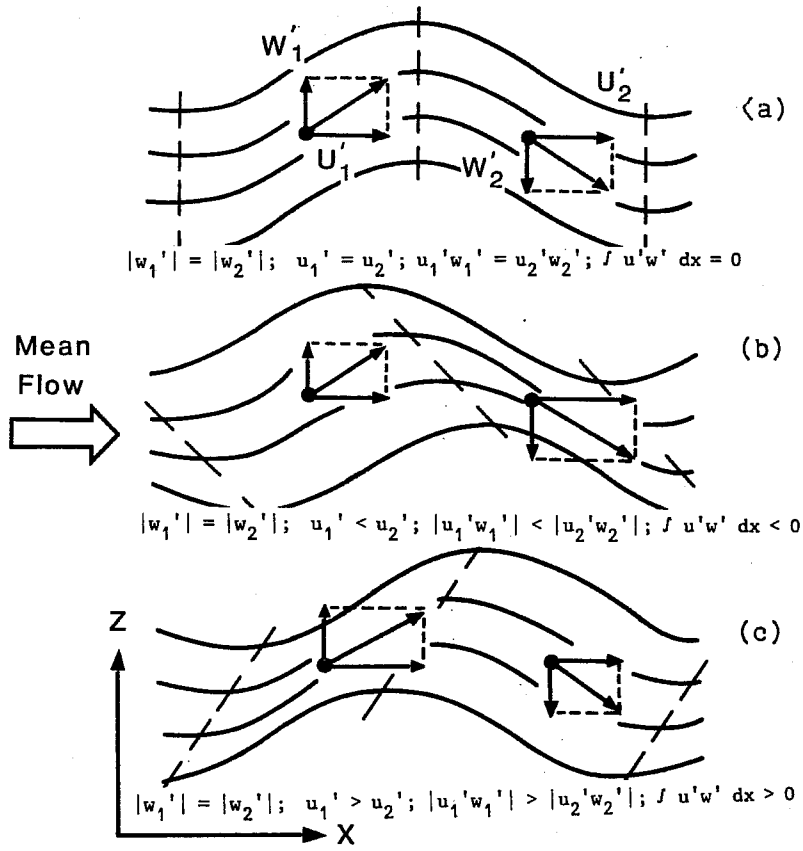

Fig.1 Vertical transfer of horizontal momentum by waves: (a) symmetrical wave; (b) wave front tilts upstream; (c) wave front tilts downstream.

Finally, it should be mentioned that Eqs.(8)-(11) are derived for two-dimensional flows. To extent these to three dimensions Eq. (2) must contain an integral over y and Eq.(3) changes to

$$\phi_o = \frac{1}{L_x L_y} \int_{L_x} \int_{L_y} \overline{\phi}\, dx\, dy. \tag{12}$$

The wave drag due to gravity-inertia waves for three-dimensional flows then changes to its component in x-direction M_x and y-direction M_y

$$\begin{aligned} M_x &= \int_{-\infty}^{+\infty} \int_{+\infty}^{-\infty} (\rho_o\, u'w')\, dx\, dy + \int_{-\infty}^{+\infty} \int_{+\infty}^{-\infty} (f\, v'\, \rho_o\, \eta)\, dx\, dy \\ M_y &= \int_{-\infty}^{+\infty} \int_{-\infty}^{+\infty} (\rho_o\, v'w')\, dx\, dy - \int_{-\infty}^{+\infty} \int_{-\infty}^{+\infty} (f\, u'\, \rho_o\, \eta)\, dx\, dy. \end{aligned} \tag{13}$$

To complete the discussion it should be mentioned that here we have neglected to so-called 'frictional drag', which represents momentum losses due to surface frictional effects.

3. THE WIND MEASURING SYSTEMS

Airborne systems can respond effectively to a wide range of scales of motion from quite long wavelengths - greater than 100 km - to turbulent eddies only a few meters long. The instrumentation intended or used for in-situ wind measurement from various aircraft has been fully described elsewhere: the british MRF-Canberra (Axford 1968), the MRF-Hercules (Nicholls 1978), the american NOAA-P3, the NCAR-Elektra and the german DFVLR-Falcon (Hauf 1984). As a brief summary, however, the main items of equipment common to most aircraft are:

- a noseboom-mounted pitot-static probe with angle-of-attack and angle-of-sideslip vanes, for measuring the airflow relative to the aircraft;
- an inertial navigation system (INS) to measure aircraft velocity relative to the ground.

INS-derived horizontal velocities are subject to drifts and long period oscillatory errors. These must be corrected by procedures which compare INS velocity components with those derived from independent measuring systems, such as surface based Doppler radar.

In general, vertical velocity can be measured in two different ways. The direct measurement principally uses air speed and the angles of pitch and attack, combined with the outputs from the inertial reference system. For

the second method of determination of vertical velocity, it is assumed that the air is flowing in steady-state two-dimensional adiabatic motion, along the mean streamlines. Details of the computation for both these methods are found in Lilly and Kennedy (1973).

Finally, we estimate the absolute accuracy and the resolution of in-situ wind measurements by airborne systems. Some values are given for specific aircraft which typify the present state of airborne measurement systems. In most aircraft the absolute accuracy of the horizontal wind speed is between 0.5 m s^{-1} (Hercules) and 1.5 m s^{-1} (FALCON), that of the vertical component is about 0.5 m s^{-1}. The relative errors are of the order of 0.1 m s^{-1}. The accuracies given above result in a noise level of 0.01 Pa for the momentum flux integral (Eq.11). However, in most cases the relative errors of the wind are some tens of cm s^{-1} leading to a noise limit between 0.05 Pa and 0.1 Pa, which is a more realistic estimate for the error level.

4. TREATING THE DATA

This section briefly discusses how to treat the data measured using the methods described in the last section, so as to obtain an estimate of momentum exchanges. We start with the unfiltered wind data as taken by the aircraft, an example is given in Fig.2 where the horizontal and vertical component of the wind is plotted along the flight tracks. The perturbation values of the horizontal wind u' and the vertical wind velocity w' are then obtained by removing the mean and any statistically significant linear trend by a least squares fitting. The mean quantity is given by the flight leg average and is similar to the quantity with the subscript 'o' in Eq.(3). In most cases it is also advisable to use a low-pass filter on the raw aircraft data to remove amplitudes of waves with horizontal wavelengths smaller than 10-20 km. This reduces the light turbulence and eliminates small-scale frequently trapped lee-waves.

The estimation of the momentum flux contains an integration over a horizontal length. Because the true ground speed of the aircraft is not constant the spatial separation of the data at an arbitrary sampling rate is also not constant. Due to this, each data point represents a particular length. To consider this, the spatial increments 'dx' are taken to be equal to 'C dt', where C is the true ground speed of the aircraft. These considerations are important for estimates of very small-scale motion, in particular for turbulence.

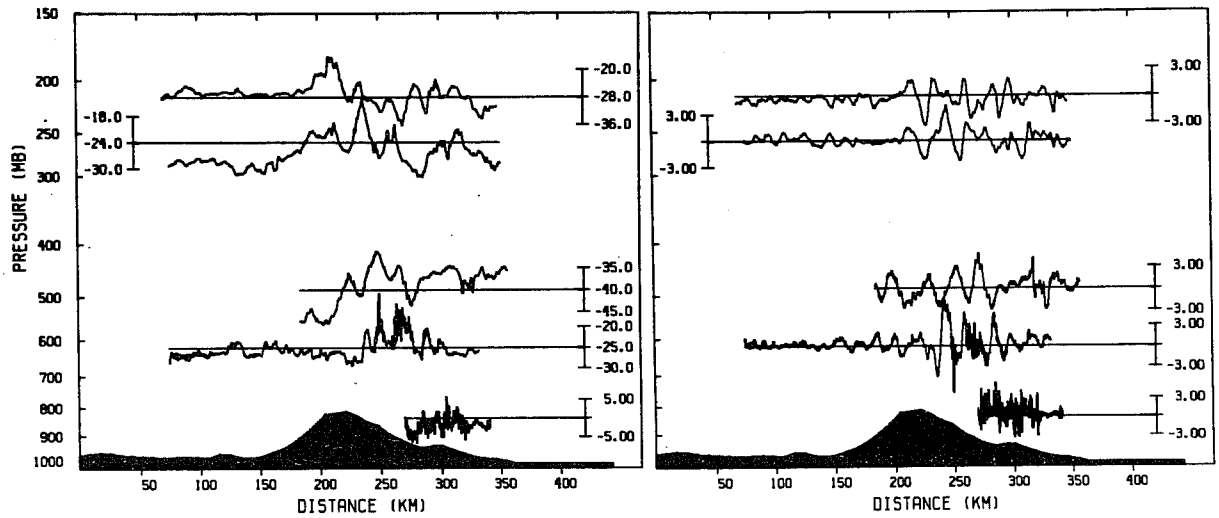

Fig.2 Aircraft measurements of southerly wind component v (left) and vertical wind components w (right) above the Pyrenees on 23/3/82. The cross-section is parallel with a line representing 2°E. The units are m s^{-1}; negative v components indicate northerly flow (Blumen and Cox 1984).

The product u'w' oscillates with an amplitude which may be a factor of 10 or 100 larger than its mean value, thus it is possible that if the sample consists of unequal numbers of up and downdraughts, Eq.(11) may give a random result. To guard against this possibility the location of major contributions to the momentum flux values can be determined by evaluating the integral

$$G(x^{\#}) = - \frac{1}{x_1 - x^{\#}} \int_{x_1}^{x^{\#}} (\rho_o \, u'w') \, dx. \qquad (14)$$

This running covariance integral $G(x^{\#})$ must be calculated along the flight traverses starting from the point furthest upstream of the mountain (x_1). An example of the results of this procedure is given in Fig.3 showing data taken from the uppermost flight leg presented in Fig.2. The running integral remains zero upstream of the mountain, dropping to -0.2 Pa above the main sink of momentum and remaining nearly constant in magnitude downstream. However, in most cases the response is not so clear, particularly in situations with trapped lee waves which are able to transport the momentum downstream over large distances.

Correlation spectra can provide some additional information on the character of the flow and its associated momentum flux. Using the filtered variables, the power spectra of u' (or v') and w' can be calculated as well as

the correlation spectra for u' (v') against w'. The u' (v') versus w' correlation is important for the determination of the momentum fluxes. Simple wave theory and observations suggest that the momentum fluxes should be negative above mountains. This is the case where the phase of u' (v') versus w' correlation spectra is between 90° and 270° with a maximum at 180° with quadrature behaviour. For phases between -90° and +90°, we expect correlations greater than zero. A positive phase < 180° signifies that the first-named variable leads the second in time.

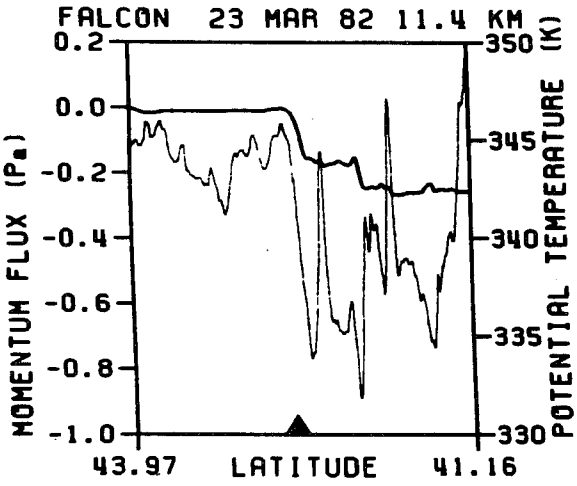

Fig.3 Running spatial integral of momentum flux (Eq.14) (thick) and potential temperature (thin) on 23 March 1982 above the Pyrenees at a height of 11.4 km (Hoinka 1984).

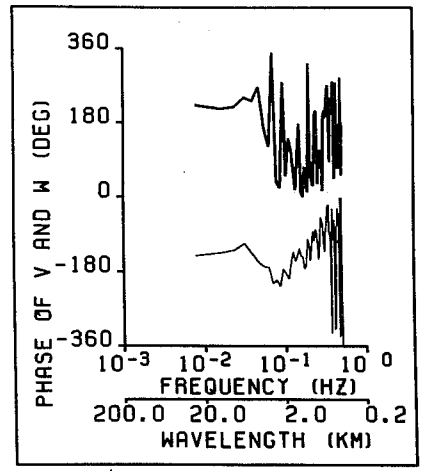

Fig.4: Phase of correlation spectrum of v' and w' for the 4.0 km flight level (thin) and 11.4 km (thick). The data were collected on 23 March 1982 above the Pyrenees (Hoinka 1984).

Fig.4 shows an example of the v' vesus w' correlation of the same event as mentioned above. Again the data are taken from the uppermost flight leg (thick line) and lowermost cross-mountain traverse (thin line) shown in Fig.2. Here, we found phases close to 180° at both levels indicating downward fluxes of horizontal momentum. The coherence level for this correlation spectrum are at 0.5 for both levels for the larger scales (Hoinka 1984). The estimated momentum fluxes for both the upper and lower level were -0.25 and -0.15 Pa, respectively (see next section). For further details on the correlation spectra, Lilly and Kennedy (1973) is recommended.

5. RESULTS OF OBSERVATIONS

In this section we summarise results from airborne measurements taking during the following experiments:

1970	Colorado Lee Wave Programme
1971	Measurements over the Colorado Rocky Mountains
1973	WAMFLEX
1976-81	Measurements over the British Isles
1982	ALPEX
1982-85	DFVLR-Foehn Experiment

During these experiments, very valuable data have been acquired with the simultaneous use of several aircraft, which allow greater vertical and horizontal sampling and less concern about temporal changes in flow structure.

5.1 The Colorado Lee Wave Programme

The principal objectives of this experiment included obtaining detailed measurements of lee waves and the associated momentum flux, in particular in flows associated with downslope windstorms in the Boulder area. The measurements were performed over the Rocky Mountains in Colorado. This mountain range is characterised by maximum heights of about 2000 m and a cross-mountain scale of about 100 km. The results of this experiment are documented e.g. by Lilly (1971), Lilly et al. (1971,1973).

The wave structure on 17 February 1970 (Fig.5) shows a moderate wave in the lower troposphere following the terrain. The unique feature appears near the very high tropopause at about 18 km, where a rapid amplification was analysed. In this region severe turbulence was generated and the flow was blocked upstream of the amplified wave. Fig.6 shows downward fluxes of 0.4 to 0.6 Pa over most of the troposphere with maxima of 0.8 to 1.0 Pa near the surface and near 18 km. These estimates are based on an averaging length of 200 km for the traverses. At a height of 18 km in the turbulent region the energy transported from below was dissipated by turbulence leading to a rapid drop-off in the vertical profile of the momentum flux.

Eliassen and Palm (1961) have shown that an upward wave energy transfer is always combined with a downward momentum flux, and that this flux is con-

stant with height for steady-state flows as long as there are no dissipative effects. For the present case an approximate constancy with height suggests that in the troposphere the vertical eddy stress ss convergence term vanishes.

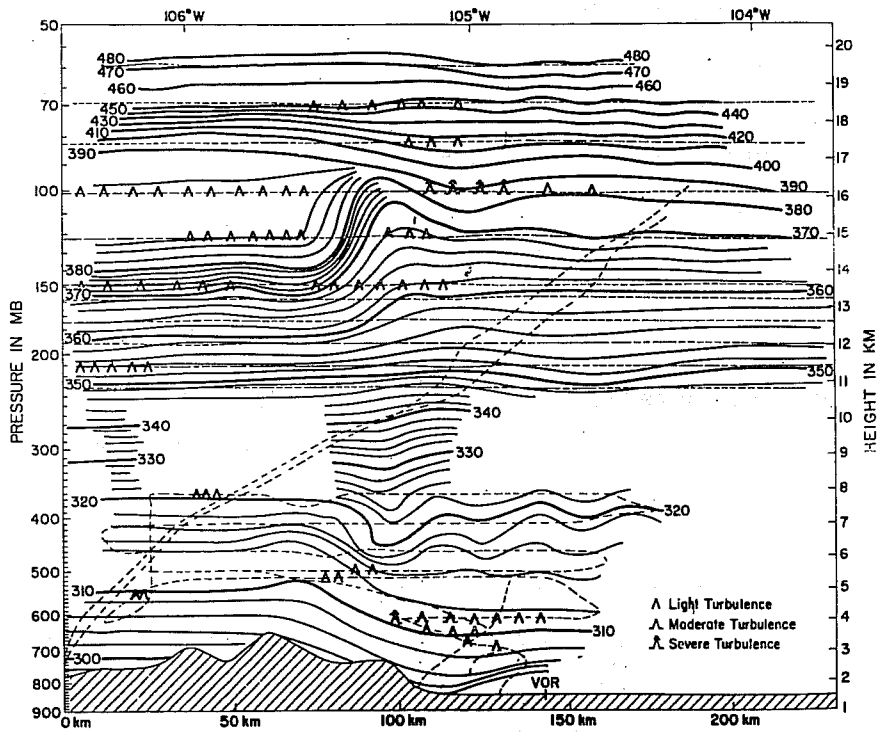

Fig.5: Potential temperature cross-section for 17 February 1970. Solid lines are isentropes (K), dashed lines aircraft or ballon flight trajectories. The cross-section is along a 275°-095° true azimuth line, crossing Kremmling (CO) and Denver VOR aircraft navigation stations (Lilly 1971).

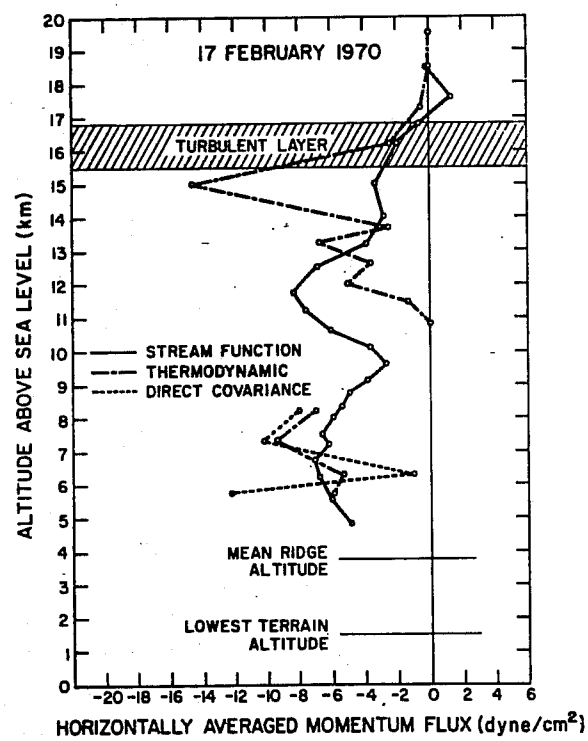

Fig.6 Mean observed profile of momentum flux (solid line) from aircraft traverses above the Colorado Rockies on 17 February 1973 (Lilly and Kennedy, 1973). The broken line shows momentum fluxes for the same upwind conditions from non-linear theory (Klemp and Lilly 1978).

5.2 Measurements over the Colorado Rocky Mountains

In 1971 a series of coordinated measurements over the Colorado Rocky Mountains were jointly performed by the NCAR, NOAA and other institutions in order to collect data during strong downslope windstorms. The results from this experiment are documented by Lilly (1978).

A very strong amplitude wave occurred over the Colorado Rockies on 11 January 1972; this event was connected with strong downslope winds (chinook up to 55 m s^{-1}) on the eastern slopes of the Rocky Mountains. Fig.7 shows an analysis of the potential temperature field. The prominent feature of this analysis is the large amplitude wave of about 6 km in the upper troposphere. Data from the 20000 and 30000 ft flight legs of 200 km used to estimate the momentum flux associated with this large-amplitude wave resulting in -4.7 Pa.

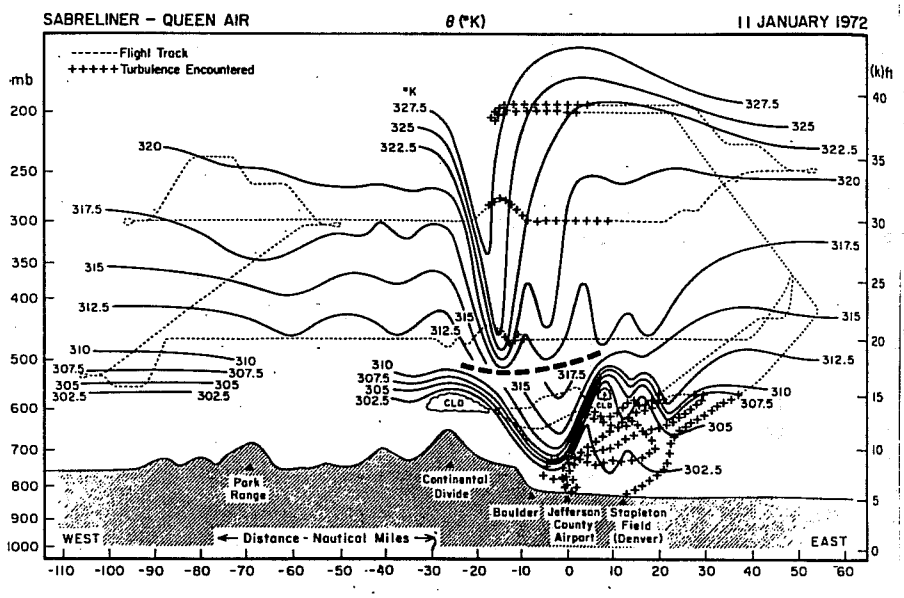

Fig.7 Analysis of the potential temperature field (solid lines) from aircraft data taken on 11/1/72. The dotted lines show aircraft tracks, with periods of significant turbulence shown by pluses (Lilly 1978).

5.3 The WAMFLEX Programme

During the winter 1973 a programme of observations, the 'Wave Momentum Flux Experiment' (WAMFLEX), was carried out in an attempt to gather a more extensive and thorough sampling of mountain waves and their associated momentum transports over the Colorado Rocky Mountains. The results of that experiment are documented by Lilly et al.(1982).

Flights were made on 20 days, summarised in Tab.1. The momentum fluxes are the average values for all flight legs flown for each day, with an averaging length of 300 km. On only three of the flight days the aircraft could measure westerly momentum fluxes of -0.1 Pa or less. The large number of flights shows the extensive effort to get a sample of data on momentum flux values and the reader can imagine how much money and manpower was required to gather these data.

Tab.1 WAMFLEX 1973 summary (Lilly et.al. 1982).

Date	Legs	Mean Momentum Flux	
		westerly (Pa)	southerly (Pa)
16/1/73	4	-0.070	-0.074
18/1/73	8	-0.400	-0.018
29/1/73	8	-0.230	-0.004
30/1/73	8	-0.063	-0.051
05/2/73	12	-0.026	+0.012
06/2/73	9	-0.053	+0.013
12/2/73	8	-0.009	+0.016
14/2/73	11	-0.026	+0.001
19/2/73	4	-0.035	-0.006
20/2/73	6	-0.093	+0.026
24/2/73	8	-0.009	-0.054
25/2/73	9	-0.051	+0.010
26/2/73	12	-0.020	+0.014
28/2/73	10	-0.028	-0.012
02/3/73	9	-0.023	0.000
06/3/73	11	-0.130	-0.021
09/3/73	10	-0.038	+0.037
12/3/73	9	-0.018	-0.034
16/3/73	4	-0.034	+0.056
20/3/73	2	-0.086	+0.139

Fig.8 shows the isentropic field analysed for the flights on 18 January 1973, the day with the strongest wave response. From the wave structure it is apparent that the primary wave response is in the form of long, nearly hydrostatic waves which propagate up into the upper troposphere. Smaller standing lee waves and transient modes are evident. Other observations (Lilly and Kennedy 1973) documented similar wave structures for large amplitude waves. These patterns of airflow are also qualitatively similar, but weaker than those described by Lilly (1978) for waves associated with an intense downslope windstorm.

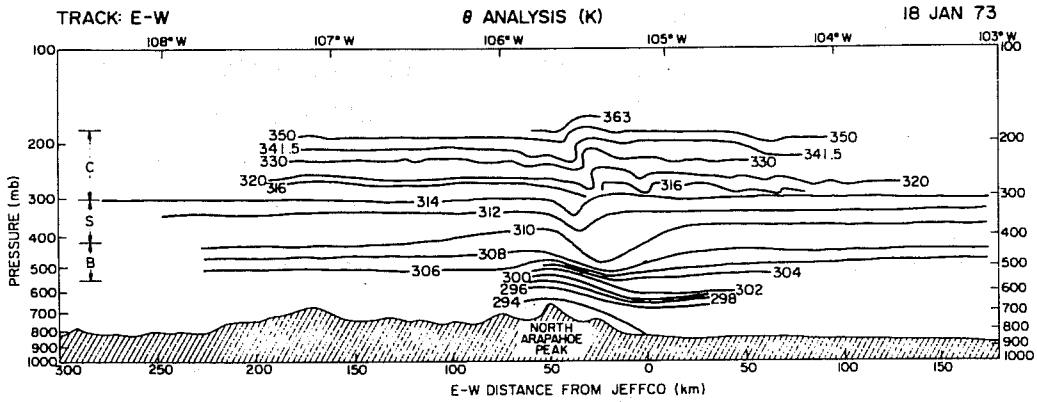

Fig.8 Analysis of the potential temperature field from aircraft flight data for 18 January 1973. The height intervals indicated on the left correspond to levels flown by various aircraft (Lilly et al. 1982).

Fig.9 (left) shows the profile of average momentum flux deduced from the results of all flights. Although the statistical sample is far from ideal, with many flights not represented at all levels, most of the amplitude arises from three days when strong waves were present, and on those days there were flights at most levels. The profile shows a fairly uniform value. Individual flights showed much larger fluctuations and average values, as exemplified by Fig.9 (right) for 18 January - the strongest case observed.

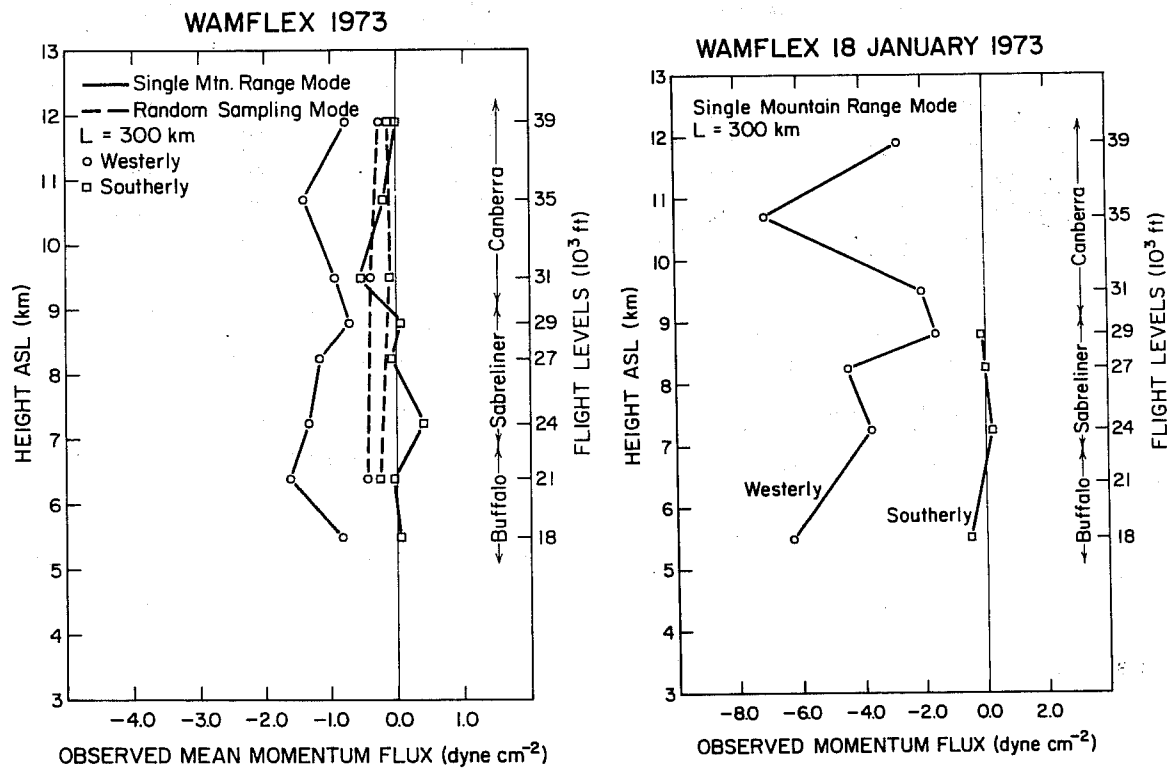

Fig.9 Profiles of momentum flux averaged over all WAMFLEX flights (left) and for the 18/1/73 flight (right) (Lilly et al. 1982).

5.4 Measurements over the British Isles

Between 1976 and 1981 several aircraft of the British Meteorological Research Flight (MRF) have made a number of flights over mountainous regions of the British Isles to investigate waves set up by mountains which are small by comparison with the Rocky Mountains. The type of underlying terrain consists of systems of ridges and valleys typically 10 km or less in width with an amplitude of a few hundred meters and extending over areas with horizontal dimensions of a few hundred kilometers. The results of this study are in Brown (1983).

The calculated momentum fluxes for several flight days are shown in Fig.10. The averaging length is 200 km. Only on two days, 8/1/81 and 12/1/76 was the magnitude of the observed fluxes greater than the noise level of the measured flux integrals. The momentum fluxes measured on 8 January 1981 have an average of -0.35 Pa. Tab.2 summarises all flights during the experiment, showing the mean values of the momentum fluxes, observed lee wave lengths and peak wave amplitudes.

Tab.2: Momentum fluxes over the British Isles (Brown 1983).

Date	Wave-length (km)	Mean Momentum Flux (Pa)	Peak Wave Amplitude ($m\ s^{-1}$)	Wind at 1 km (deg)	($m\ s^{-1}$)
18/7/80	9.6	-0.01	0.9	280	12.9
3/12/80	10.9	-0.02	2.0	355	12.8
20/6/80	11.6	-0.07	1.7	280	15.5
12/1/76	18.3	-0.10	2.2	290	25.1
08/1/81	20.9	-0.35	2.4	245	30.5

The direction of the flight patterns were designed for wave fields which are two-dimensional, that is having no variation in the direction perpendicular to the background wind. The low-level wind directions of all cases are given in Tab.2. The authors discussed the relation between the upstream soundings representing the background flow and the resulting wave structure and its associated momentum flux. However, the impact of different orographic forcing due to different flight patterns was not discussed.

Using linear theory Brown (1983) has attempted to relate the measured momentum fluxes to the wavelength and degree of trapping of the lee waves. He identified two distinct categories of lee wave motion. The first type with wavelengths around 10 km which are strongly trapped, as shown by a

large 1/e decay lengths (> 1000 km) were characterized by small mean values of the momentum flux between -0.01 and -0.1 Pa. For the second type, with a rather long lee-wavelength of around 20 km and a decay length of about 100 km indicating relatively weakly trapping, the corresponding momentum flux is -0.35 Pa. In general, large values of momentum flux appear to be associated with long, weakly trapped lee wave modes.

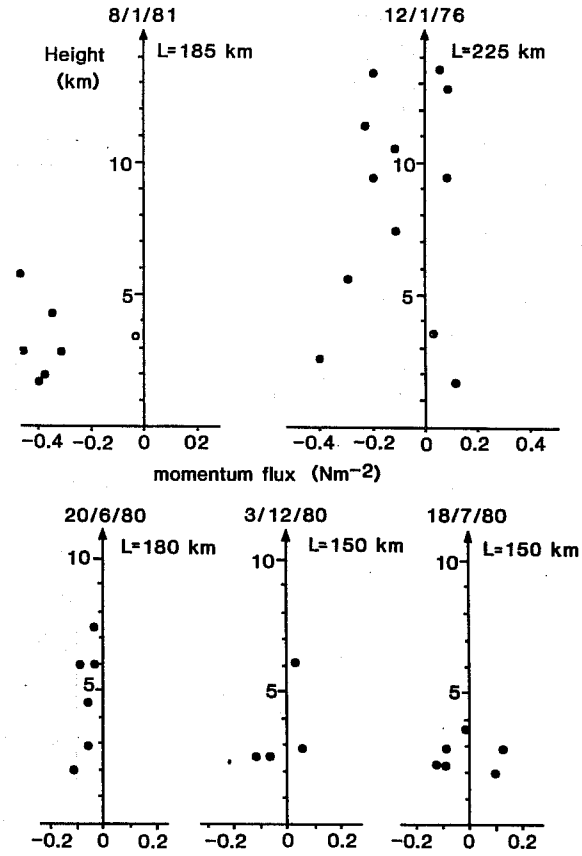

Fig.10 Measurements of the vertical flux of horizontal (along wind) momentum above the British Isles on 8 January 1981, 12 January 1976, 20 June 1980, 3 December 1980 and 18 July 1980 (Brown 1983).

5.5 ALPEX

The 'Alpine Experiment' (ALPEX) was designed to provide a dataset of measurements over and in the vicinity of the Alps. The scientific tasks for ALPEX included the study of the drag of the mountain complex upon the atmosphere; the vertical transport of horizontal momentum as function of height near the mountain range; and the dissipation of gravity-inertia wave energy over and downwind of the mountain range.

During ALPEX, the atmosphere refused to co-operate in providing cross-mountain flow situations associated with substantial momentum exchanges between the mountain and the atmosphere. However, a strong mountain wave event occurred above the Pyrenees during the ALPEX period. The wave event

over the Pyrenees is documented by Blumen and Cox (1984), Hoinka (1984, 1986), Cox (1986). The Pyrenees are located at the border between France and Spain touching the Mediterranean Sea as well as the Atlantic Ocean. The approximate mean height is 2000 m, maximum height is 3200 m.

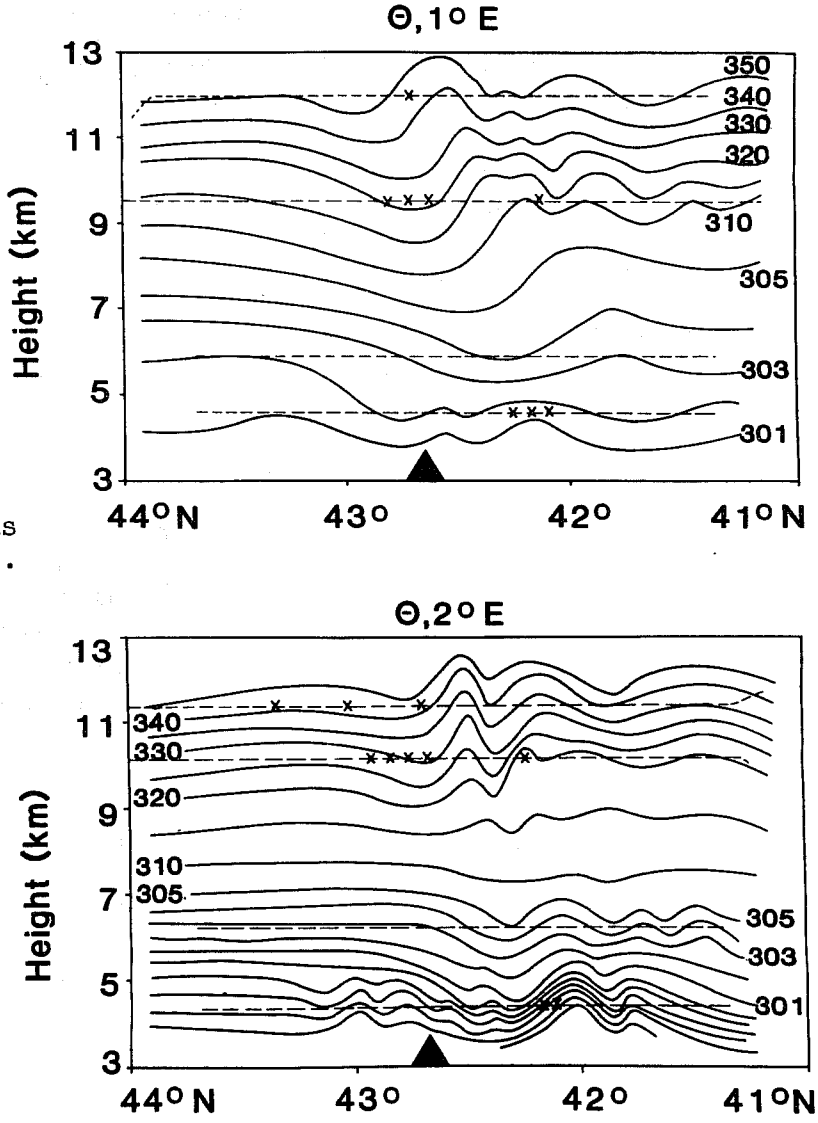

Fig.11 Cross-sections of potential temperatures in K along a north-south line between 44°N and 41°N for March 23, 1982. The top (bottom) figure shows the structure along 1° (2°) E. The dashed lines indicate the flight legs. The black triangle indicates the approximate location of the main ridge of the Pyrenees. The crosses mark regions where light turbulence was encountered (Hoinka 1984).

Fig.11 shows the analysed isentropic field of two cross-sections, one parallel to 1°E and the other to 2°E. The 2°-section is similar to that presented in Fig.2 showing wind data. In both cases, a northerly flow (from the left) without waves approaches the barrier. At the lee side in the layer between 6 and 12 km, similar wave patterns were analysed for both cross-sections, which were about 80 km apart. In the lower troposphere, there are remarkable differences between both sections. In the 1°-section only one wave is visible, while there are small-scale lee waves in the 2°-section. The phaselines tilt upstream in the vertical indicating a downward flux of horizontal momentum.

Fig.12 shows the vertical profile of the momentum fluxes. The averaging length for the evaluation of the momentum fluxes was 300 km. A similar profile is evaluated by Cox (1986). Due to general uncertainty and noise of momentum flux integrals, it was appropriate to average the upper four estimates and the lower four estimates to obtain representative estimates for both layers. In the present case there is a vertical divergence in the momentum fluxes. This seems not to be an effect of the combination of two profiles measured 80 km apart because both profiles have a similar shape. In the real airflow over the Pyrenees there are dissipative effects, so one should not expect strong constancy with height. Fig.12 either shows the inapplicability of the steady-state assumption (Eliassen and Palm 1961) or demonstrates simply that the flight legs were not long enough to allow clear separation of mean and fluctuating velocity, or both.

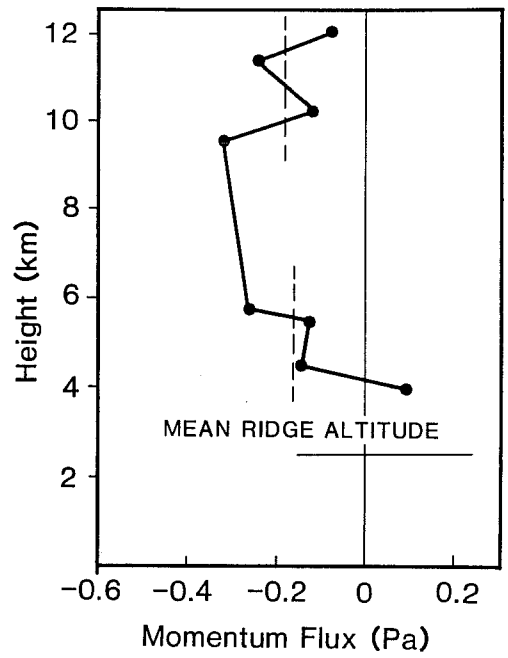

Fig.12 Observed profile of momentum flux obtained over the Pyrenees on March 23, 1982. The broken lines represent averaged values over the upper and lower four estimates (Hoinka 1986).

5.6 The DFVLR Foehn Experiment

One aim of ALPEX was to study the dynamical and thermal structure of the troposphere above the Alps during foehn. However, weather conditions during ALPEX were unco-operative in providing foehn events. So, between 1982 and 1985 a field programme took place in southern Germany conducted by the DFVLR to investigate the mesoscale structure of foehn and to determine the momentum exchange between the Alps and the overlaying troposphere during strong cross-mountain flow. Some results of this field experiment are documented in Hoinka et al. (1984) and Hoinka (1985). The Alps are oriented roughly west to east, extend for 500 km, their north to south scale is about 100 km with averaged heights of about 2000 m and their maximum heights are around 3500 m.

The isentropic fields observed on 11 November 1982 are given in Fig.13 (top). A waveless flow approaches the Alps from the south. Analysis shows a double wave with a wavelength of 60 km above the barrier at a hight between 6 and 12 km. The phaselines are tilted vertically upstream, indicating a downward flux of horizontal momentum. In the lower troposphere on the lee side above Innsbruck (bottom figure), there is a wave of wavelength of approximately 50 km with an amplitude of 1-2 km. This wave is associated with small-scale lee waves. During this strong foehn event the isentropes above Innsbruck show hydraulic jump behaviour similar to those observed above Denver (Fig.7) during strong chinook, but with lower amplitude.

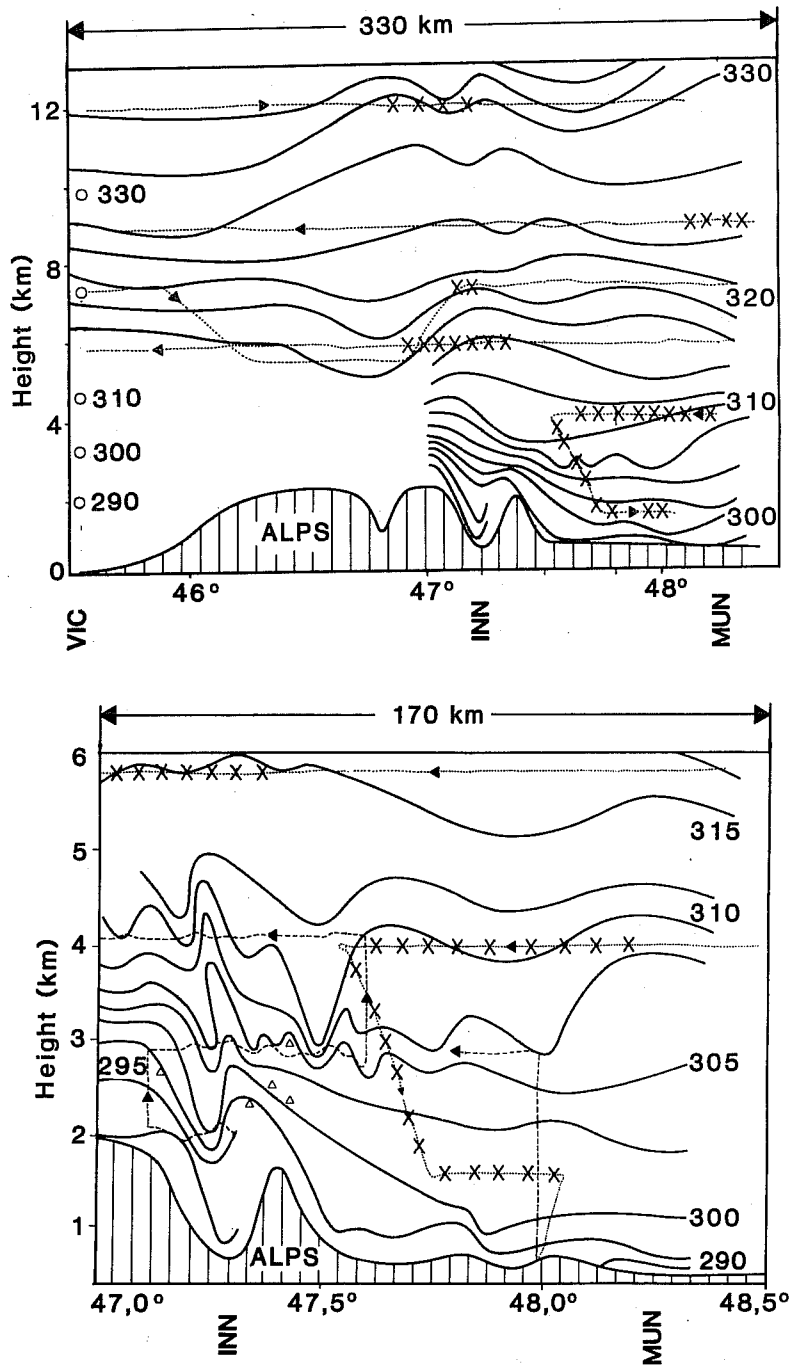

Fig.13 Cross-sections of potential temperatures in K along a north-south line between Munich (MUN) and Vicenza (VIC) on 8/11/82. The bottom figure shows the enlarged cross-section between Innsbruck (INN) and Munich. The dotted lines indicate the flight legs and the crosses mark regions where light to moderate turbulence were encountered (Hoinka 1985).

In Fig.14 the vertical fluxes of meridional, latitudinal momentum and a combination of both are given. The averaging length is 300 km. At all levels of the troposphere the fluxes are negative, as would be expected from mountain wave theory. The magnitude of the flux of westerly momentum is close to 0.1 Pa, that of the southerly flux is between 0.1 and 0.3 Pa and that evaluated using wind speed is between 0.2 and 0.3 Pa.

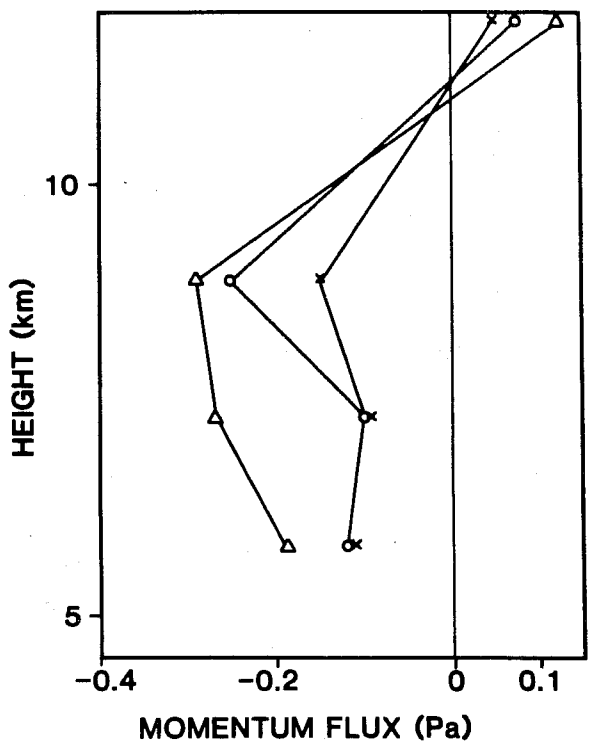

Fig.14 Profiles of wave momentum flux measured on 8 November 1982. The southerly (westerly) fluxes are indicated by circles (crosses). The flux values evaluated using wind speed are given by triangles (Hoinka 1985).

Flights were made on 4 days with moderate to strong south-foehn (summarised in Tab.3). The momentum fluxes are the averaged values for all flight legs flown for each day, with an averaging length of 300 km. On only one of the flight days the aircraft could measure negative westerly and southerly fluxes. The results indicate that the correlation between cross-mountain flow, foehn and momentum flux is not clear for the Alps at present.

Tab.3 DFVLR-Foehn-Experiment summary.

Date	Legs	Mean Momentum Flux	
		westerly (Pa)	southerly (Pa)
08/11/82	4	-0.099	-0.175
24/11/82	4	+0.016	+0.011
26/11/82	4	+0.064	+0.009
07/05/85	4	-0.040	+0.009

5.7 Summary

A summary of significant momentum flux values derived from observed data is given in Tab. 4. All values are estimated using Eq.(11). At present no estimates of the complete wave drag including the net Coriolis force have been calculated. As mentioned above, the additional drag would be about 20% in the Alps and even less in the Rocky Mountains. However, for these mountains this supplementary part is close to the noise level of the data, in particular in moderate momentum exchange cases.

Tab.4 Summary of cross-mountain momentum flux values derived from observed data.

	Momentum flux (Pa)	Domain Size (km)
Rocky Mountains (17/2/70)	-0.60	200
Rocky Mountains (11/2/72)	-4.70	200
Rocky Mountains (18/1/73)	-0.40	300
British Isles (8/1/81)	-0.35	200
Pyrenees (23/3/82)	-0.20	300
Alps (8/11/82)	-0.20	300

A further component of the drag force acting between the earth and the atmosphere is the frictional drag. The relative importance of this drag is illustrated by its magnitude of -0.2 Pa (for winter 45°N) assuming 300 km for the length of the forcing region (Kung, 1968). The magnitude of the observed wave drags (Tab.4) corresponds closely to the frictional drag. But there is no information about whether these two types of drag are correlated, perhaps inversely, which would lead to a partial compensation.

Because sampling flights are very expensive, it is not possible to perform field experiments everywhere or for extended periods. Mesoscale models are an powerful tool in simulating airflow over mountains and for evaluating the momentum flux due to gravity waves. Lilly et al. (1982) attempted to correlate the magnitude of the observed wave momentum flux during WAMFLEX with the computed values from the Klemp-Lilly model (Fig.15). The version of wave theory used to derive fluxes for comparison with observations is linearized, steady state, inviscid, two-dimensional and uses a simplified terrain shape. The predicted values are about four times too large. Nevertheless, although the model only considers simple types of flow, the data agree reasonably well with the theoretical predictions.

Another way of getting momentum flux estimates without measuring in-situ is described by Lilly et.al. (1982). Most situations with significant momentum flux values are connected with strong wave activity above and in

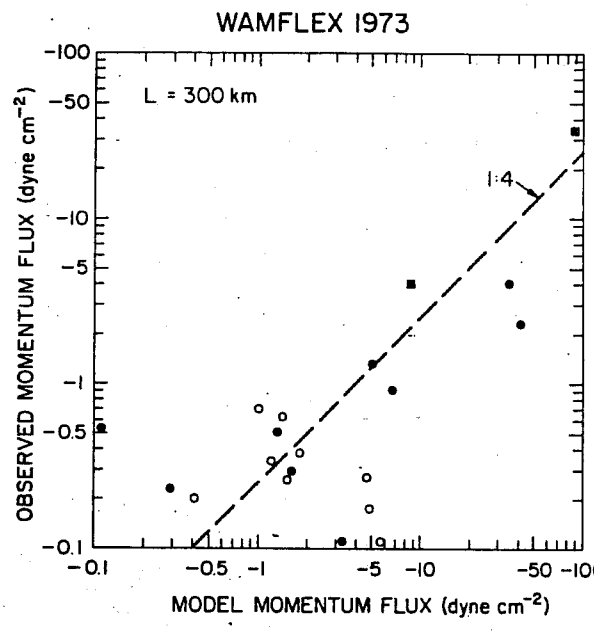

Fig.15 Average observed momentum flux from WAMFLEX flights versus computed values from the Klemp-Lilly model. The open circles represent random sampling flight modes, while the solid circles represent single mountain range flight modes. The solid squares are additional data points from strong wind cases: 17 February 1970 and 11 January 1972 (Lilly et.al. 1982).

the lee of the mountains. These situations are in turn frequently associated with strong downslope wind events, foehn, chinook and bora which usually occur with strong surface pressure gradients across the mountains (foehn nose). In Fig.16 the magnitude of the observed momentum flux is compared with the magnitude of the surface wind speed in the lee of the mountains. Additionally we have plotted available values for European airflow over mountain events. The remarkably good correlation shows the close link between downslope winds and wave amplitude and suggests that surface anemomentry may, in some cases, be a substitute for the much more expensive aircraft measurements in evaluating the momentum flux.

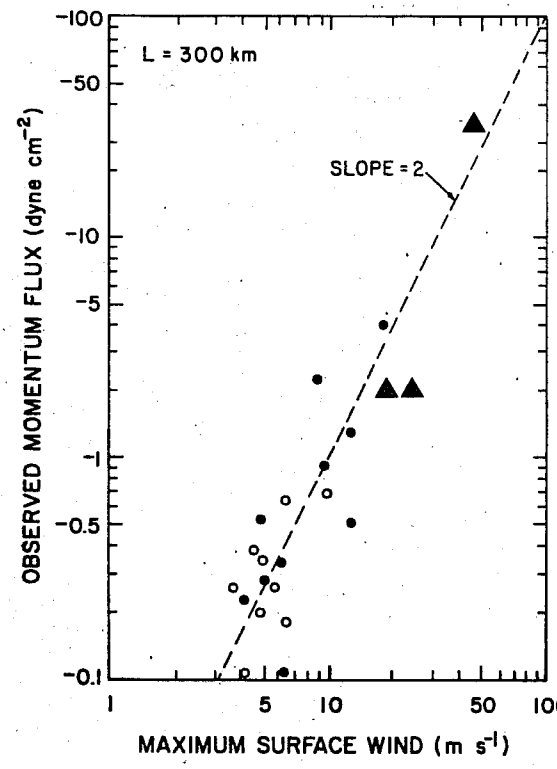

Fig.16 Mean observed momentum flux values from WAMFLEX flights versus maximum wind gusts observed in Boulder, Colorado. The open circles represent random sampling flight modes, while the solid circles represent single mountain range flight modes. The triangles are additional data points from strong wind cases: 11/1/72 (Wind/Boulder), 8/11/82 (Wind/Innsbruck), 23/3/82 (Wind/Jaca).

Lilly et al. (1982) pointed out that this comparison was much more successful than that between the aircraft data and the pressure difference across the Front Range as measured by a pair of microbarographs. The latter measurements failed to give reasonable results - especially the weak wave cases. In Tab.5 cross-mountain pressure gradients, lee side wind measurements and observed momentum fluxes are given for several wave events. The pressure gradients for the 11/1/72 event are evaluated using the difference over a distance of 20 km (a) and 40 km (b) across the Continental Divide.

Tab.5 Surface pressure gradient, wind and momentum flux data.

		Surface Pressure (10^{-2} mb km^{-1})	Foehn ($m\ s^{-1}$)	Momentum Flux (Pa)
Rocky Mountains (11/1/72)	(a)	≈55	55	-4.70
	(b)	≈35	55	-4.70
Pyrenees (23/3/82)		?	20	-0.20
Alps (8/11/82)		10	25	-0.20

Recently, surface pressure drag estimates were computed using an array of microbarograph stations aligned across the Alps (Davies and Phillips 1985) and from synoptic pressure data (Hafner and Smith 1985). It would be interesting to compare surface drag values derived with these methods with momentum fluxes estimated from aircraft data in order to prove if it is possible to use these cheaper methods instead of the more expensive of aircraft methods.

6. THE MOMENTUM FLUX DUE TO TURBULENCE

Above mountainous terrain, moderate to severe turbulence is encountered six times more often than over plains and ocean (McPherson and Morrissey 1971) (Fig.17). It is clear that this mountain generated turbulence also has a role to play in the momentum budget and must be seen in connection with the mountain wave generated momentum flux.

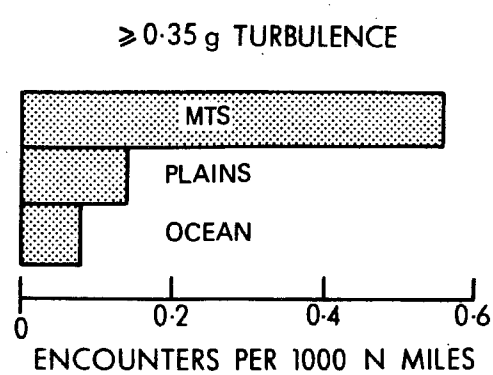

Fig.17 Relative frequencies of moderate or severe turbulence over mountainous terrain compared to that over flat terrain and the ocean. Measurements were made during flights of about 40 000 nautical miles over each of the three surface types mainly at 12.8 km (McPherson and Morrissey 1971).

During most observations reported in the last section, there was moderate to severe turbulence. An example is the event shown in Fig.5 where the worst turbulence was confined to levels at and below the mountain tops, and to the stratosphere, especially between 15 and 18 km where the ambient shear was disorted by large-scale pertubations in the airflow.

Linear lee wave theory (Bretherton 1969) suggests that a turbulent layer should essentially absorb the wave energy of an impinging upward propagating gravity wave and prevent its further upward propagation. The 17/2/70 case (Fig.5) shows this characteristic behaviour. In another case a mid-tropospheric turbulence zone originates in a region of intense wave-generated shear and is then carried downstream by the mean flow and upward by the motion (Fig.7).

Since waves interact weakly with turbulence in a nonlinear way, and only then under certain conditions, initially they can be considered to be distinct from turbulence even though they are usually present together (Busch 1969). Eq.9 defines the momentum flux due to turbulence. This flux depends strongly on the definition of the characteristic scales Δx, Δz and Δt. An ideal specification of the increments would be a gap in the energy spectrum implying that the atmospheric flow is clearly separably into mean and turbulent components that are uncoupled in the sense of suppressed interactions. Based on the location of the gap, the data can be separated into means and deviations, both of which are functions of time (or space).

Finally, budget terms can be computed assuming that the overbar in Eq.(2) implies low-pass filtering of the particular quantity and the star represents high-pass filtering. In practice, the cut-off frequency cannot always be placed in a gap. In the absence of some sort of spectral gap, the selection of the region at which separation should occur is arbitrary. An apparent gap often shifts its position in frequency space as a function of the size of the sample analysed and the spatial position of the sample with respect to the area of strong turbulence.

There are not many studies of observations of turbulence associated with mountain waves. Two studies, Lilly (1978) and Lester and Fingerhut (1974), deal with the turbulence during the strong downslope wind event on 11/1/72 (Fig.7). A region of intense turbulence was encountered on the east of the

main trough region at about 2 km above and a few kilometers downstream of the crest of the mountains. The turbulence generated in this region was probably carried by the updraught to the tropopause. Lilly (1978) analysed data from the 6 km flight leg. The sampling rate was either 4 or 8 s^{-1} corresponding to about 40 or 20 m of ground track. The most intense turbulence occurred at 6 km and lasted for about 90 s, or 15 km of ground track.

Lilly (1978) analysed a strongly positive momentum flux in the turbulence region (Fig.18, right). The corresponding running covariance integrals for the entire flight leg of 200 km (Fig.18, left) show that the total momentum flux is of opposite sign to the contributions from the turbulence zone. This strongly suggests, but does not prove, that without the high-frequency turbulence components the momentum flux would be substantially larger than its observed net value. The spatial scale of the turbulence differed substantially from that of the driving wave. Lilly found that the integrated momentum flux in the turbulence zone was about 360 x 10^3 N m^{-1} (≡1.8 Pa).

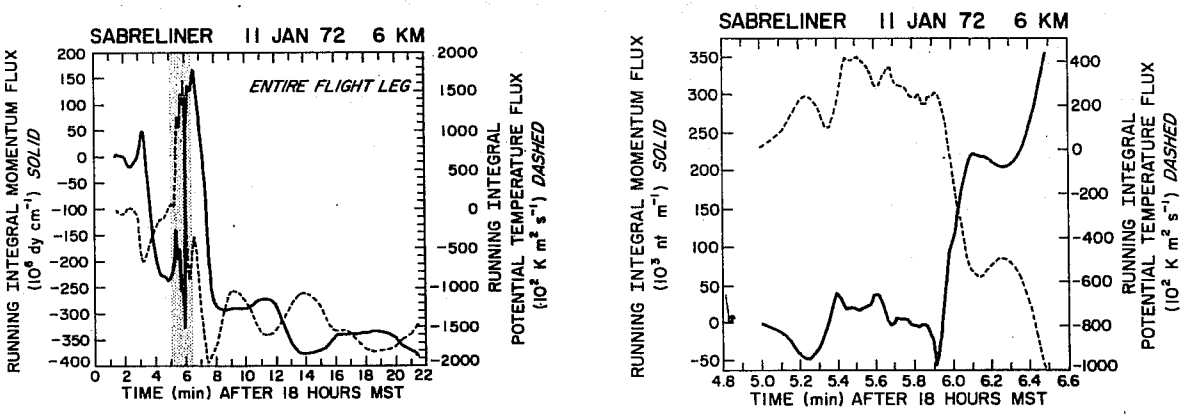

Fig.18 Running spatial integral of momentum flux $\int \rho_0 u'w'dx$ (solid) and temperature flux (broken) over the entire 6 km flight leg (left) and over the turbulence zone of this leg (right) (Lilly 1978).

Lester and Fingerhut (1974) studied the characteristics of the lower turbulence zone which is frequently associated with mountain lee waves. The estimated dissipation rates based on horizontal gust velocities are of the order of 20-100 W m^{-2} (≈0.001-0.03 $m^2 s^{-3}$). These values were found to be typical for the lower turbulent zone of a mean depth of 3 km. Lilly (1978) pointed out that this turbulence was probably generated by surface roughness, augmented by shears developed in the separation region, and then carried aloft to a height of 2-3 km.

Dissipation rates of the order of 24 W m^{-2} (≈0.1 m^2s^{-3}), averaged over a 200 km interval, were observed for the airflow over the Rocky Mountains event on 17/2/70 (Fig.5) in the strong turbulence zone at 100 mb (Lilly 1971). Above the Pyrenees the observations gave dissipation rates of about 0.03 m^2s^{-3} (Hoinka 1984) and above the Alps during foehn they were of the order of 0.02 m^2s^{-3} (Hoinka 1985). For the strong turbulence event on 11/1/72 Lilly (1978) obtained dissipation rates of the order of 1.0 m^2s^{-3}, showing the very great rate of energy removal.

7. SUMMARY AND PROBLEMS

In this section we summarise problems with the measurement and evaluation of the momentum flux using data measured in-situ by aircraft and outline future work. Perhaps the most unsatisfying results of all of the observational programmes relates to the net effect of mountain waves on their small-scale, meso-scale and larger-scale environment, in particular the location and mode of exchange between wave and mean state momentum fluxes. In general, the problems are due to the fact that real flows are unsteady, three-dimensional, rotational and are associated with frictional and diabatic processes.

In most studies it has been assumed that the whole wave field remains stationary with respect to the ground for the duration of the experimental part of the flight, which is a reasonable assumption in some cases although there is some doubt in others. Analysis indicates that roughly the same pattern also prevails on a larger scale, though at the meso-scale, the flow can certainly not be considered either stationary or two-dimensional.

Real flow and orographic forcing is three-dimensional. Over the Rocky Mountains the upstream flow at levels well below the mountain-top is sometimes blocked and diverted northward, mostly passing through the gap in the Continental Divide in central Wyoming, while what arrives at the surface in eastern Colorado has been above 3 km since entering the north American continent. An even more complicated situation is encountered in the European Alps. How is it possible to estimate the momentum flux due to gravity-inertia waves in these complicated flow events and how can the streamlines be determined in these three-dimensional situations? For the Alps it is not clear what the real momentum flux is for a diagonal cross-mountain flow, e.g. from Marseille towards Munich.

Real mountain ranges are always finite horizontally, which is often difficult to define simply and it is thus difficult to define the up and downstream region of influence. Laboratory studies emphasise that mountains may have an influence upstream. Observations show that the mean state is often irreversibly altered up and downstream by passing over a major mountain range. Consider, for example, the case of 11 January 1971, where the observed wave momentum flux was enormous, amounting to about 4.7 Pa. A cursory inspection of Fig.7 reveals large changes in temperature between the up and downstream ends, evidently associated with a net downward displacement of most of the tropospheric air stream. Analysis shows similar behaviour in cross-mountain flow over the Pyrenees (Fig.11) and the Alps (Fig.13). This might be regarded as due to not observing the flow far enough up or downstream. There must, in fact, be considerable doubt as to the meaning of the calculation of wave momentum flux when it is based on deviations from a mean state defined by a least squares trend line between arbitrarily located up and downstream points.

The difference in behaviour between perfectly trapped and leaky lee wave modes has implications for the actual measurements of wave momentum flux. As the wave becomes more strongly trapped so the disturbance will reach further downstream. Under these circumstances, the momentum flux obtained from fixed length runs may underestimate the total drag on the mountain. The measurements would also be expected to be more noisy as the mean momentum flux becomes a smaller fraction of the amplitude of the oscillations of u'w'.

It is well known that mountains affect the atmosphere, causing clouds and rain by forcing the air to rise and to become cooler. Which role do diabatic processes play? Numerical studies show that the wave drag changes, as soon as humitidy processes becomes important. Does humidity or cloud reduce or reverse the drag? What are the effects of rain or snow on mountain waves? In general, the dynamics of moist waves are not understood well enough.

There is still uncertainty about the effect of turbulent breakdown on the wave structure and its associated momentum flux, especially where there are critical layers. For flows associated with severe turbulence, such as hydraulic jumps, it is unclear how to determine the momentum exchange. How much wave momentum is transfered to smaller turbulence-scale momentum and

is finally dissipated? The interaction of waves and turbulence needs further theoretical study and observation.

Clearly, as Lilly (1972) suggests, far more work needs to be done in the future to clarify the role of gravity and gravity-inertia waves generated by mountains, in particular on the energy and momentum budgets of the atmosphere. Since only a small number of well-defined cases of airflow over mountains have been obtained, more are needed in order to determine the representativeness of the existing data, in particular for the Alps. Measurements will have to be taken daily over mountains for a long period.

As well as the airborne in-situ-measurement systems, several remote-sensing systems have been developed in the last 10 years to measure the wind field: Doppler-radar, Laser-Doppler-anemometer and VHF-radar. These systems should be used in the near future to estimate momentum fluxes generated by mountains. Furthermore, the results of calculating surface pressure drag using microbarograph data or synoptic pressure data should be compared to momentum fluxes estimated using data measured from aircraft.

ACKNOWLEDGEMENT:
Karl W. Cox is thanked for pointing out an error in my paper (Hoinka 1984)

REFERENCES:

Axford, D.N., 1968: On the accuracy of wind measurements using an inertial platform in an aircraft, and an example of a measurement of the vertical mesostructure of the atmosphere. J.Appl.Meteor., 7, 645-666.

Blumen, W. and K.W. Cox, 1984: Lee-waves over the Pyrenees; data, analyses and chronicle; 21-23 March 1982. Report Department of Astrophysical, Planetary and Atmospheric Sciences, University of Colorado, Boulder USA.

Bretherton, F.P., 1969: Momentum transport by gravity waves. Quart.J.R. Met.Soc., 95, 213-243.

Brown, P.A., 1983: Aircraft measurements of mountain waves and their associated momentum flux over the British Isles. Quart.J.R.Met.Soc., 109, 849-865.

Busch, N.E., 1969: Waves and turbulence. Radio Sciences, 4, 1377-1379.

Cox, K.W., 1986: Analysis of the Pyrenees lee wave event of 23 March 1982. Mon.Wea.Rev., 114, 1146-1166.

Davies, H.C. and P.D. Phillips, 1985: Mountain drag along the Gotthard Section during ALPEX. J.Atmos.Sci., 42, 2093-2109.

Eliassen, A. and E. Palm, 1961: On the transfer of energy in stationary mountain waves. Geofis.Publ., 22, 1-23.

Hafner, T.A. and R.B. Smith, 1985: Pressure drag on the European Alps in relation to synoptic events. J.Atmos.Sci., 42, 562-575.

Hauf, T., 1984: Turbulenzmessungen mit dem Forschungsflugzeug Falcon. Meteorol.Rdsch. 37, 163-176.

Hoinka, K.P., 1984: Observation of a mountain-wave event over the Pyrenees. Tellus 36A, 369-384.

Hoinka, K.P., 1985: Observation of the airflow over the Alps during a foehn event. Quart.J.Roy.Met.Soc. 111, 199-224.

Hoinka, K.P., 1986: Corrigendum to 'Observation of a mountain-wave event over the Pyrenees'. Tellus 38A, 93-94.

Hoinka, K.P. and H. Fimpel, H. Peters, H. Willeke, 1984: Data Catalog for the 1982 DFVLR Observational Foehn Experiment. DFVLR-FB 84-33, 146p.

Klemp, J.B. and D.K. Lilly, 1978: Numerical simulation of hydrostatic mountain waves. J.Atmos.Sci., 35, 78-107.

Kung, E.C., 1968: On the momentum exchange between the atmosphere and the earth over the northern hemisphere. Mon.Wea.Rev., 96, 337-341.

Lester, N.E. and W.A. Fingerhut, 1974: Lower turbulent zones associated with mountain lee waves. J.Appl.Met., 13, 54-61.

Lilly, D.K., 1971: Observations of mountain-induced turbulence. J.Geophys.Res., 76, 6585-6588.

Lilly, D.K., 1972: Wave Momentum Flux - A GARP Problem. Bull.Amer.Met. Soc., 53, 17-23.

Lilly, D.K., 1978: A severe downslope windstorm and aircraft turbulence event induced by a mountain wave. J.Atmos.Sci., 35, 59-77.

Lilly, D.K. and P.J. Kennedy, 1973: Observations of a stationary mountain wave and its associated momentum flux and energy dissipation. J.Atmos. Sci., 30, 1135-1152.

Lilly, D.K. and J.M. Nicholls, R.M. Chervin, P.J. Kennedy, J.B. Klemp, 1982: Aircraft measurements of wave momentum flux over the Colorado Rocky Mountains. Quart.J.R.Met.Soc., 108, 625-642.

Lilly, D.K. and Y. Pann, P. Kennedy, W. Toutenhoofd, 1971: Data catalog for the 1970 Colorado Lee Wave Observational Program. NCAR Technical Notes, Boulder Co. USA.

McPherson, J.I. and E.G. Morrissey, 1971: Stratospheric turbulence and temperature change measurements from the Coldscan project. London, Proc. R.Ae.S/AIAA/CASI International Conf. on Atmospheric Turbulence May, 1971.

Nicholls, S., 1978: Measurements of turbulence by an instrumented aircraft in a convective atmospheric boundary layer over the sea. Quart.J.R.Met. Soc., 104, 653-676.

Smith, R.B., 1979: The influence of the earth's rotation on mountain wave drag. J.Atmos.Sci., 36, 177-180.